RSC Advances

ROYAL SOCIETY OF CHEMISTRY

www.rsc.org/advances

Impact of structural stability of cold adapted *Candida antarctica* lipase B (CaLB): In relation to pH, chemical and thermal denaturation

Gulam Rabbani[1], Ejaz Ahmad[1], Mohsin Vahid Khan[1], Mohd. Tashfeen Ashraf[2], Rajiv Bhat[3] and Rizwan Hasan Khan[1*]

[1] Interdisciplinary Biotechnology Unit, Aligarh Muslim University, Aligarh-202 002, India
[2] School of Biotechnology, Gautam Buddha University, Greater Noida-201308, India
[3] School of Biotechnology, Jawaharlal Nehru University, New Mehrauli Road, New-Delhi 110067, India

[*]**Address for correspondence:**

Interdisciplinary Biotechnology Unit
Aligarh Muslim University,
Aligarh 202 002, India
Telefax: +91-571-2721776
E-mail: rizwanhkhan@hotmail.com, rizwanhkhan1@gmail.com

Running Title: Characterization of molten globule state

Abbreviations: ANS: 1-anilino-8-napthalene sulfonate; CaLB: *Candida antarctica* lipase B; C_m: midpoint concentration; ΔC_p: change in excess heat capacity; DLS: Dynamic light scattering, DSC: differential scanning calorimetry; GuHCl: guanidine hydrochloride; ΔG_u^o: Change in unfolding free energy in the absence of denaturant; ΔH_{cal}: change in calorimetric enthalpy; ΔH_{vH}: change in van't Hoff enthalpy; MG: molten globule; MRE: mean residue ellipticity; SEC: size exclusion chromatography; T_m: midpoint temperature.

Abstract

Effect of pH on the conformational behavior of *Candida antartica* lipase B (CaLB) has been monitored by spectroscopic and calorimetric studies. The results obtained from far and near-UV CD, intrinsic fluorescence and ANS binding studies indicate that CaLB exhibits the characteristic properties of a molten globule in acidic (protonated) condition at pH 1.4. The molten globule state retained about 67% of its secondary structure with a substantial loss of tertiary structure at pH 1.4. Moreover, equilibrium unfolding studies indicated that the 'molten-globule-like' state unfolds in a non-cooperative manner and is thermodynamically less stable than that of native state. The molten globule possessed a slightly higher R_h than its native state. DSC thermogram shows a high heat signal at pH 7.4, while low heat signal at pH 2.6, and suggests that CaLB is likely to have undergone structural changes during the thermal unfolding. However partially unfolded CaLB at pH 1.4 do not produce a DSC peak which proves the existence of molten globule state at pH 1.4 as supported by spectroscopic data. The Stokes radius of the MG state obtained by SEC experiments is found to be 33% larger than the native state, but essentially smaller than the denatured state.

Keywords: Cold adapted lipase, *Candida antarctica* lipase B, DLS, DSC, guanidine hydrochloride denaturation, molten globule, refolding.

1. Introduction

Lipases (EC 3.1.1.3) catalyze the hydrolysis of triglycerides to form glycerol and fatty acids. They are versatile enzymes that are distributed throughout living organisms. Cold adapted lipases are largely distributed in microorganisms existing at low temperature, around 5 °C. Although a number of lipase producing sources are available, but few bacteria and yeast have been exploited for the production of cold adapted lipases [1]. Cold adapted enzymes are characterized by higher activity at low and moderate temperatures when compared to their mesophilic counterparts and therefore have attracted considerable interest in industrial processes as energy savers by elimination of cooling cost [2], in industrial food or feed technologies [3] and in detergent industry as additives [4]. The identification of mechanisms by which cold adapted enzymes achieve extraordinary efficiency at low temperatures is always a topic of utmost investigation[5].

However, environmental adaptation of proteins at low temperatures is much less understood [6]. It is quite difficult to diagnose the structural features that are answerable for cold adaptation because critical changes for thermal adaptation are hidden amid those produced by evolutionary pressure (Supplementary Fig S1). Various adaptation strategies have been proposed that the current accepted hypothesis favors that cold adapted enzymes are more flexible, with a reduced number of stabilizing interactions [7]. The increased flexibility is needed to execute catalysis at low temperatures to endorse easy binding and transformation of the substrate, thus compensating the freezing effect in cold habitats. In many cold adapted enzymes the increase in global or local structural flexibility is coupled with low stability [8], however, it has also been shown that activity and stability are not always inversely correlated. Reports are available that interprets the mechanism and

effectiveness of cold adapted enzyme shows stability similar or even higher than that exhibited by their mesophilic counterparts [9].

Attempts have been made from time to time to isolate cold adapted lipases from these microorganisms having high activity at low temperature. The lipases have been used as biocatalysts for the hydrolysis of a large number of synthetic substrates. Under properly chosen conditions, the reaction is reversible and so lipases can also be used for esterification. Their versatility has led to the frequent use of lipases as biocatalysts at the industrial-scale for the production of fine chemicals and pharmaceuticals, and as additives in household detergents [10].

Candida antarctica lipase B (CaLB) is a monomeric protein which consists of 317 amino acid residues with dimensions of 30×40×50 Å (Fig 1), It is a multitryptophan (Trp52, 65, 104, 113 and 155) and multityrosine (Tyr61, 82, 91, 135, 183, 203, 234, 253, and 300) containing protein, as shown in Fig 1. It belongs to the α/β-hydrolase fold family with a conserved catalytic triad consisting of Ser, Asp/Glu and His, a characteristic feature of all serine hydrolases [11]. The active site of CaLB shares the common catalytic triad Ser105-Asp187-His224, however, unlike most lipases, it has no lid which covers the entrance to the active site and so do not show interfacial activation [12]. It is an efficient catalyst for hydrolysis in water and esterification in organic solvents [13].

It is used in many industrial applications because of its high enantioselectivity, wide range of substrates, thermal stability and stability in organic solvents [14]. The enzyme maintains its activity in organic solvents and is used for various applications including polymerization, resolution of alcohols and amines, modifications of sugars and sugar related compounds, desymmetrization of complex drug intermediates and ring opening of β-lactams [15]. The pH optimal for CaLB is at pH 7.4, with rapid fall in activity below pH 6.0 and above pH 8.0. This loss in activity is usually explained by the ionization state of

Asp187 and His224 residues of the catalytic triad. The cold adapted lipases are equipped with a very low proportion of Arg as compared to Lys. A small hydrophobic core, lesser number of Pro and very small number of salt bridges and aromatic-aromatic interactions are associated with cold adapted lipase. In this regard, the weakening of hydrophobic clusters, the decrease in Pro content (40%) and ratio of the Arg/Arg+Lys make lipases active even at low temperature [16]. Protein folding studies indicate a discrete pathway with the formation of intermediate states between native and denatured states [16, 17]. The molten globule state which is characterized by a compact denatured form of protein that retained a significant amount of native-like secondary structure, but a largely disordered tertiary structure with the exposure of buried hydrophobic regions of the protein transition [19]. The molten globule exists as an intermediate between native and denatured state [18]. The role of molten globule as a functional entity in protein folding has been hypothesized, and further evidence has also shown that this state is involved in several biological processes such as membrane insertion, trans-membrane trafficking, and chaperone assisted refolding which require the protein to be partially unfolded [20].

The present report describes the structural detail of circular dichroic (CD) and fluorescence studies on the stability of the secondary as well as tertiary structures of CaLB to different pH and guanidinium hydrochloride (GuHCl). Dynamic light scattering (DLS) and size exclusion chromatography (SEC) measurements were also carried out and results were correlated with the structural stability of the enzyme. In order to understand the pH-dependent thermal stability of CaLB, differential scanning calorimetric (DSC) and far-UV CD thermal unfolding studies at different pH conditions were undertaken. DSC measured the thermodynamic parameters such as calorimetric enthalpy (ΔH_{cal}), van't Hoff enthalpy (ΔH_{vH}) and the changes in excess heat capacity (ΔC_p) which contribute towards the conformational stability and were used to compare the physical and biological properties

of the enzyme. This finding is particularly significant, just because the studied enzymes possess a flexible and strictly conserved scaffold in solution.

2. Materials and methods

Recombinant lipase from *Candida antarctica* lipase B (62288), thioflavin T (ThT), guanidine hydrochloride (GuHCl), 4-*p*-nitrophenyl butyrate (4-*p*-NPB) and 1-anilinonaphthalene-8-sulfonate (ANS) were purchased from Sigma Chemical Co. All other reagents used in the study were of analytical grade.

The pH induced unfolding studies of CaLB were carried out in 20 mM of KCl-HCl (pH 0.8-1.6), Gly-HCl (pH 1.8-3.0), sodium acetate (pH 3.5-5.0), sodium phosphate (pH 6.0-8.0), Gly-NaOH (pH 9.0-10.0) and KCl-NaOH (11.0-13.0) buffers. Each buffer was passed through a 0.45 μm filter before making solution.

8 M GuHCl stock solutions were prepared at pH 7.4, 2.6 and 1.4 in 20 mM solutions of the above mention buffers and further pH of GuHCl solution was adjusted with addition NaOH solution. Protein samples were incubated for 12 h at room temperature in different pH before spectroscopic measurements were recorded.

2.1. Protein concentration determination

Stock of CaLB was prepared in 20 mM sodium phosphate buffer, pH 7.4 and its concentration determined from the value of molar extinction coefficient (ε_M) = 40,690 M^{-1} cm^{-1} at 280 nm by using molecular weight of 33 kDa [21].

2.2. Circular dichroic measurements

CD measurements were carried out with a Jasco spectropolarimeter (J-815) equipped with a Peltier-type temperature controller (PTC-424S/15). The instrument was calibrated with D-10-camphorsulphonic acid. Spectra were collected in a cell of 1 and 10 mm pathlength

and protein concentrations used were 6 and 30 μM for far- and near-UV CD respectively. The scan speed was 100 nm min^{-1} and response time of 1 s for all measurements. Each spectrum was the average of 2 scans. The raw CD data obtained in millidegrees were converted to mean residue ellipticity (MRE) in deg cm^2 $dmol^{-1}$ which is defined as

$$\mathrm{MRE} = \frac{\theta_{\mathrm{obs}}(m\,\mathrm{deg})}{10 \times n \times C \times l} \qquad (1)$$

where, θ_{obs} is the CD in millidegrees, n is the number of amino acid residues (317-1= 316), l is the path length of the cell in cm and C is the molar concentration of CaLB. The helical content was calculated from the MRE values at 222 nm using the following equation as described by Chen et al [22]:

$$\%\alpha\text{-helix} = \left(\frac{\mathrm{MRE}_{222\,\mathrm{nm}} - 2{,}340}{30{,}300}\right) \times 100 \qquad (2)$$

Furthermore, we used K2D3 program from European Molecular Biology Laboratory (EMBL) as additional analysis to authenticate the Chen et al method for secondary structure content. Furthermore, deconvolution of the CD spectra provides the estimate of other secondary structure present in CaLB.

The thermal unfolding of CaLB was evaluated by measuring the temperature-dependent CD response at 222 nm from 30 to 95 °C using a temperature slope of 1 °C min^{-1}. The chemical denaturation experiment was done by equilibrating individual samples of CaLB (6 μM) with varying GuHCl concentrations (0-6 M) at pH 7.4, 2.6, 1.4 respectively for 12 h at 25 °C.

2.3. Data analysis of protein denaturation

Chemical and thermal denaturation data from CD and fluorescence spectroscopy were analyzed on the basis of a two-state unfolding model. For a single step unfolding process,

N⇄U, where N is the native state and U is the unfolded state, the equilibrium constant K_u is

$$K_u = \frac{f_u}{f_n} \quad (3)$$

where f_u and f_n are the fraction of U and N, respectively.

$$f_d = \frac{(Y_{obs} - Y_n)}{(Y_u - Y_n)} \quad (4)$$

where, Y_{obs}, Y_n and Y_u represent the observed property, the property of the native state, and the property of unfolded state respectively.

The change in free energy of unfolding in water ΔG_u^o is obtained by the linear extrapolation model [23]. The relationship between the denaturant and ΔG_u^o is approximated by the following equation:

$$\Delta G_u = -RT \ln K_u \quad (5)$$

and

$$\Delta G = \Delta G_u^o - m(D) \quad (6)$$

where, m is the experimental measure of the dependence of ΔG_u on denaturant concentration, R is the gas constant (1.987 cal K^{-1} mol^{-1}) and T is absolute temperature.

2.4. Turbidity measurements

The turbidity of protein samples under different conditions was measured by recording absorbance at 350 nm on Perkin-Elmer Lambda 25 double beam UV-Vis spectrophotometer. The measurements were carried out at 25 °C in a cuvette of 1 cm path length. The CaLB concentration was 6 μM.

2.5. Rayleigh light scattering and thioflavin T (ThT) fluorescence measurements

Rayleigh light scattering measurements were performed on a Hitachi spectrofluorometer, (F-4500). The fluorescence spectra were measured at 25 °C with a 1 cm pathlength cell. Protein samples are incubated under desired pH conditions were excited at 350 nm and the intensity of the scattered light was recorded at 350 nm.

A stock solution of thioflavin T (ThT) was prepared in double distilled water. The concentration of ThT determined by using molar extinction coefficient of (ε_M) = 36000 M^{-1} cm^{-1} at 412 nm. Protein samples of 6 μM at different pH were incubated in 1:3 molar ratio of ThT for 30 minutes at 25 °C. The fluorescence of ThT was excited at 440 nm. The spectra were recorded from 400 nm to 600 nm.

2.6. Tryptophanyl fluorescence measurements

The fluorescence was measured by exciting the protein at 280 nm and emission spectra were recorded in the range of 300-400 nm. The excitation and emission slits were set at 5 and 10 nm respectively. The CaLB concentration was 6 μM.

2.7. ANS binding measurements

A stock solution of ANS was prepared in distilled water and its concentration was determined using molar extinction coefficient of (ε_M) = 5,000 M^{-1} cm^{-1} at 350 nm. For ANS binding experiments, the molar ratio of protein to ANS was 1:10. The excitation wavelength was set at 380 nm and the emission spectra were observed in the range of 400-600 nm. Both the excitation and emission slits were set at 10 nm. The CaLB concentration was 6 μM.

2.8. Acrylamide-quenching experiments

In the fluorescence quenching experiments, aliquots of 2 M quencher stock solution were added to protein solutions (6 μM) to achieve the desired range of quencher concentrations (0.02-0.1 M). Excitation wavelength was set at 295 nm in order to excite Trp residues only,

because acrylamide itself absorbs at 280 nm. The emission spectrum was recorded in the range 300-400 nm. The decrease in fluorescence intensity was analyzed by using the Stern-Volmer equation:

$$\frac{F_o}{F} = 1 + K_{sv}[Q] \quad (7)$$

where F_o and F are the fluorescence intensities of CaLB in absence and presence of quenchers. K_{sv} is the quenching constant which was determined from the slope of the Stern-Volmer plot at lower concentrations of quencher, whereas [Q] represents molar concentration of quencher.

2.9. In vitro unfolding and refolding of CaLB

The protein unfolded in 20 mM sodium phosphate buffer pH 7.4, containing 4 M GuHCl for 2 h. The unfolding of CaLB was monitored by loss of enzymatic activity, far-UV CD, tryptophan and ANS fluorescence. Refolding was initiated by rapid dilution of GuHCl denatured protein in refolding buffer, which was the same as unfolding buffer without GuHCl. Refolding mixture was then incubated at 25 °C for 1 h, and the refolding yield was calculated from enzymatic activity recovered by the refolded protein in 1 h as a percentage of native protein. Final protein concentration in the refolding buffer was always kept less than 5 μM. Refolding was initiated by rapid dilution of denatured protein in refolding buffer to different final GuHCl concentrations while maintaining the final protein concentration at 0.25 μM, manual mixing. Refolding kinetic traces were monitored by measurement of the change in tryptophan fluorescence at 322±1 nm. The excitation wavelength was 280 nm, and the excitation and emission slit width were set at 3 nm. The time-dependant changes in fluorescence intensity ($FI_{322\ nm}$) were satisfactorily described by double exponential kinetics:

$$f = f_o + A_1 e^{-x/t_{fast}} + A_2 e^{-x/t_{slow}} \quad (8)$$

where f is fluorescence intensity at infinite time, f_o is initial fluorescence intensity, k_{fast} and k_{slow} is the rate constant, $t_{1/2fast}$ and $t_{1/2slow}$ are half time of decay expressed in sec.

2.10. Dynamic light scattering measurements

DLS measurements were carried out at 830 nm by using DynaPro-TC–04 dynamic light scattering equipment (Protein Solutions, Wyatt Technology, Santa Barbara, CA) equipped with a temperature-controlled microsampler. Before measurement, all the solutions were spun at 10,000 rpm for 10 min and filtered through a microfilter (Whatman International, Maidstone, UK) with an average pore size of 0.22 µm directly into a 12 µl black quartz cell and the protein concentration was 30 µM. Measured size was presented as the average value of 20 runs. All data were analyzed by using Dynamics 6.10.0.10 software at optimized resolution. The mean hydrodynamic radii (R_h) and polydispersity were estimated on the basis of an autocorrelation analysis of scattered light intensity data based on translational diffusion coefficient (D) by the Stokes-Einstein equation:

$$R_h = \frac{kT}{6\pi\eta D_w^{25°C}} \quad (9)$$

where, R_h is the hydrodynamic radius, k is the Boltzman's constant, T is the absolute temperature, η is the viscosity of water and $D_w^{25°C}$ is translational diffusion coefficient.

2.11. Size-exclusion chromatography

To determine the Stokes radius of CaLB at different pH conditions, size-exclusion chromatography (SEC) experiments were carried out on a Sephacryl S-200 column ($r \times l$ = 1.0 cm × 45.0 cm, Borosil). The column was pre-equilibrated with desired respective buffers. Blue dextran was used to determine the void volume of the column. The elution was carried out under a flow rate of 14 ml h^{-1} and the absorbance of eluted fractions was monitored at 280 nm. The Stokes radii were determined by analysis of the elution volume

with respect to a calibration curve prepared as previously described by [24]. There were 6 standard proteins used for the calibration curve cytochrome *c* (17 Å), lysozyme (19 Å), ovalbumin (30 Å), bovine serum albumin monomer (36 Å) and dimer (43 Å), conalbumin (39 Å) and glucose oxidase (52 Å). 1 ml of approx 30 μM CaLB samples was loaded on to the column.

2.12. Differential scanning calorimetry

Thermal denaturation experiments were conducted on a VP-DSC microcalorimeter (MicroCal, Northampton, MA). The DSC scans were run between 20 and 90 °C at a rate of 1.0 °C min^{-1}. The experiments were performed using 10 μM CaLB incubated at room temperature for 12 h in desired pH and the reference cell contained respective buffer. The respective reference scan was run under identical DSC set up conditions and was subtracted from each sample scan. The heat capacity curves, midpoint temperature (T_m), calorimetric enthalpy (ΔH_{cal}), and van't Hoff enthalpy (ΔH_{vH}) were analyzed using Origin 7.0 software.

3. Results

3.1. Far-UV CD studies

Fig 2A depicts far-UV CD spectra of CaLB at pH 7.4, 2.6, 1.4 and in the presence of 6 M GuHCl. CaLB at pH 7.4 is characterized by two negative minima at 208 and 222 nm respectively, which is the characteristic feature of α-helix. Under the native pH conditions, the helical content is about 32%±1.0 which is in agreement with the helical content seen in the crystal structure of CaLB (34%) [25]. Most of the spectral features of native state were retained at pH 2.6, suggesting the presence of 48% secondary structure. This is also evident from the calculated % α-helical content of protein (Table 1). At pH 2.6, the minima at 208 and 222 nm were reduced and it adopts a typical appearance of a random

coil structure with emergence of a strong negative peak at around 200 nm, indicates the loss of secondary structure [26]. At pH 1.4, CaLB forms random coil like structures, with a deep minimum in the 200-210 nm range. The denatured state of protein (6 M GuHCl) appeared to have lost all elements of secondary structure. Fig 2B shows the continuous decrease in the negative MRE_{222} of CaLB with variation in pH from 7.0 to 13.0 and pH 7.0 to 1.0 suggesting that enzyme continuously losing its secondary structure. Thus there are four phases as determined by the change in $MRE_{222\ nm}$ with variation in pHs. In the first phase major structural alterations were observed between pH 13.0 to 11.0. In the second phase i.e from pH 11.0 to 4.0, there is no significant change in the negative $MRE_{222\ nm}$ indicating it is structurally more stable zone for CaLB. In the third phase (pH 4.0 to 2.0), a sudden fall in the negative $MRE_{222\ nm}$ can be observed while in the fourth phase (pH 2.0 to 1.0) there is a little increase in $MRE_{222\ nm}$. This suggests that the secondary structure of CaLB has been altered below pH 4.0. The helical content were calculated according to the Chen et al method [22] (equation 2) and presented in Table 1. According to the data presented in Table 1, we conclude that the native CaLB possess 32±1.0% α-helix while at pH 1.4 it decreases from 32±1.0% to 24±1.2%. Thus, the overall structural change in CaLB was highly pH dependent. Further, we run K2D3 program for prediction of secondary structure composition that was more accurate than that of Chen et al method [22]. The secondary structure of CaLB was calculated by, K2D3 program yielding 33±1.5, 20±1.2 and 23±1.4% α-helix at pH 7.4, 2.6, 14 respectively. As expected the other secondary structure such as β-sheet and random coil (RC) displayed a pH dependent change that accompanied by decrease in α-helix (Table 1). At pH 2.6, CaLB achieved the highest level of RC, approximately 66±1.4%, which is about 1.3 fold higher than that of native CaLB. Overall, our far-UV CD result allow us to conclude that the CaLB undergoing α-helix to RC transition during acid induced unfolding.

3.2. Effects of different pH values on near-UV CD spectra of CaLB

For the better understanding of the pH induced modifications in the local environment of aromatic amino acid residues, we performed near-UV CD measurements of CaLB. The near-UV CD spectrum of CaLB at pH 7.4 reveals three positive peaks at 283, 280 and 276 nm respectively (Fig 3A). Native state of protein revealed a broad maxima around 272-280 nm arising from Phe and Tyr side chains and a trough at 285 nm contributed by Trp residues. The peak at 277 nm is more pronounced in the native structure, a characteristic of buried aromatic chromophores particularly Tyr residues. A significant decline in MRE $_{277\ nm}$ was noticed below pH 4.0 and above pH 9.0 (Fig 3B). The differential changes observed at 277 nm might be due to change in the aromatic environment as a result of the loss of tertiary interactions. Under similar conditions, all the spectral features of CaLB in the presence of pH 1.4 and 6 M GuHCl indicates the loss of tertiary structure. This proportional loss in near-UV CD signals corresponds to the contribution of the partially unfolded state of CaLB. MGs are generally distinguished by a dramatic loss of near-UV CD signal [27].

3.3. Far and near-UV CD measurement for efficient refolding of CaLB induced by acidic and basic buffer

The refolding sample solution was dialyzed twice against a 20 mM sodium phosphate buffer pH 7.4, at 4 °C to minimize the possible effects of the unfolded state. We performed refolding experiments with the acid and basic-unfolded protein. The refolding experiments were performed in the range of pH 1.0-13.0 and changes were monitored by far and near-UV CD (Fig 2A and 3A). Adjustment of pH of the protein incubated at pH 1.0 back to pH 7.4 and further incubated at pH 11.0 back to pH 7.4 resulted in formation of a different secondary structure of the protein (Fig 2A). Below the pH 1.0 and above the pH 11.0, negligible recovery of the secondary structure indicates that the CaLB remains unfolded

under extreme pH conditions. Conversely, it retained ~60% of the initial secondary structure at pH 7.4, suggesting that the enzyme is either more stable or immediately refolds under the assay condition. Between pH 2.0 to 5.0, the CD spectrum changed to that of native like CaLB immediately after the pH jump (spectra not shown in figure). Thus, acid unfolded CaLB was found to refolded to the native like state via a simple increase in the pH to >5.0. However, at pH 5.0, subsequent aggregation occurred upon further incubation at 25 °C, causing a decrease in ellipticity. Considering that the theoretical isoelectric point (pI) of CaLB is 5.8, instability at pH 5.5-6.0 is an intrinsic property independent of the refolding via acid unfolding. The composition of the acid refolded secondary structure (from pH 1.0 to 7.4) was estimated to be: 90%, showing partial reformation of the secondary structure.

A further increase in pH from 7.4 to 12.0 drove the CD signal towards the unfolded conformation of the protein, and the CD signal showed a red shift to 205 from 202 nm. There was a rapid unfolding when the pH was raised to 10.0 and the enzyme showed little structural organization above this value. Increase in pH upto 11.0 resulted in loss of the secondary structures, and at pH 12.0 the enzyme had lost structural organization with negligible CD signal. The alkali refolded secondary structure content (from pH 11.0 to 7.4) showing 84% partial reformation of the secondary structure.

The partial reorganization of the tertiary structure of CaLB was observed in near-UV CD region (Fig 3A). The enhanced exposure of hydrophobic amino acids was reversed to the extent of native like state of protein (Fig 3A). Adjustment of pH of the protein incubated at pH 1.0 back to pH 7.4 displays a large negative band, with two minima at 277 and 282 nm. Alkali refolding from pH 11.0 back to pH 7.4 resulted in re-formation native like tertiary structure.

3.4. Turbidity measurements for determination of aggregate formation of CaLB

Turbidity measurement was performed by taking absorbance at 350 nm of CaLB at different pH conditions. The absorbance values of the samples at 350 nm are very low and lie between 0.05 to 0.2 arbitrary units. Interestingly, low value of absorbance at 350 nm indicated that no aggregate formation takes place under different pH conditions (Fig 4A). However, increase in turbidity at pH 5.0 may also be the result of isoelectric point (pI) of CaLB which lies between pH 5.0 and 8.0 [28]. A significant increase in turbidity was observed at pH 12.0, may be due to CaLB hydroxylation. Overall, at different pH, the turbidity was insignificant and almost similar at all pH values.

3.5. Rayleigh light scattering (RLS) and ThT fluorescence measurements for determination of aggregate formation of CaLB

Light scattering at 350 nm is another parameter used to determine the extent of aggregate formation. The changes in scattering of CaLB at 350 nm at different pH values are shown in Fig 4B. The variation in pH do not cause appreciable changes in light scattering of the CaLB at either below or above neutral pH (Fig 4B). This suggests that CaLB resists aggregate formation under both acidic and alkaline conditions. At pH 5.0, CaLB shows an enhanced scattering because of its isoelectric point which lies between pH 4.0 to 8.0 [28]. However, the scattering due to aggregation of protein was not observed at pH 1.4 which could be due the charge repulsion.

To check the possibility of aggregation of CaLB incubated at pH range from 1.0 to 13.0, ThT binding assay was performed. Fig 4B shows the ThT fluorescence intensity at 480 nm (subtracted from appropriate blanks) of CaLB at different pH values. CaLB at pH 1.0 to 9.0 had lowest fluorescence intensity, slight increase in FI at 480 nm above pH 9.0 due to the hydroxylation of ThT. Cundall et al argued that ThT get hydroxylated ($ThTOH^-$) in alkaline solutions (pH 10.0-12.0) and proposed existence of theoretical ThT structure [29]. Moreover, Fodera et al concludes that sensitivity and reliability of ThT in alkaline

condition is not suitable for aggregate detection [30], as in case of CaLB, the unusual increment in ThT fluorescence intensity in alkaline condition cannot be correlated with presence of aggregates. The RLS and ThT binding experiments suggest that there is no aggregate formation during the pH denaturation.

3.6. Recovery of CaLB after unfolding and enzyme kinetics

The influence of pH was determined by monitoring the well-established hydrolase activity of CaLB. The activity of lipase was studied in incubated preparation of CaLB in different pH buffers (pH 1.0-13.0) to monitor the changes in hydrolase activity by described protocol of Rabbani et al [18]. The lipase was stable in the range from pH 6.0 to 8.0. But samples incubated in lower and higher pH buffer is associated with a discernible reduction in the hydrolase activity of CaLB, which may be connected to the unfolding of the native protein structure. The results indicate that this enzyme presents an optimal activity at pH 7.4. The enzyme retains 80% of its activity at pH 8.0, but only 78% at pH 9.0, 75% at pH 6.0, and only 43% at pH 5.0 respectively (Table 2). The activity at higher pH values (pH 12.0) was not tested because of spontaneous hydrolysis of 4-*p*-NPB [22].

We quantitatively assessed the refolding yield based on the amount of soluble proteins recovered. After the refolding from the acid and alkali-unfolded state, recovered protein indicating that CaLB remained soluble at each refolding step (Table 2). The recovery of enzymatic activity was calculated from the retained activity of refolded CaLB with respect to pH 7.4. Taken together, CaLB can be partially refolded via acid and alkali-unfolding by a simple refolding procedure in terms of secondary structure and enzymatic activity and protein recovery.

Further it is seen that below and above pH 7.4 activity consecutively decreases with decrease and increase in pH. The higher value of K_m 4.05×10^4 μM for CaLB at pH 7.4 indicates the binding affinity of substrate or activity with enzyme inhibited as compared to

the CaLB at below and above pH 7.4. The large decrease in K_m indicated that the conformational changes are occurring in tertiary and secondary structure of CaLB as confirmed by the far and near-UV CD measurements. In addition to, the alteration in pH affected the steric hindrance exerted by the limitation of the substrate accessibility to the active site of this lipase. The catalytic efficiency value, which is the ratio of k_{cat} over K_m was also different for different pHs. As shown in Table 2, the lower the value k_{cat}/K_m ratio means, the poorer the enzyme works on that substrate. A comparison of k_{cat}/K_m ratio for the same enzyme with substrates in different conditions is widely used as a measure of enzyme effectiveness.

3.7. Tryptophanyl fluorescence

Intrinsic fluorescence analysis was used to understand the conformational transitions that affect the tertiary structure of protein. The pH induced microenvironmental changes around aromatic residues of CaLB were studied by monitoring the changes in fluorescence spectra (Fig 5A). The λ_{max} of CaLB under native condition (pH 7.4) was found to be 322±0.69 nm (Table 3), suggestive of high number of Tyr residues and burial of the Trp residues which were in the hydrophobic core of the protein under native condition. This observation is consistent with the reported crystal structure of CaLB (Fig 1). Fully water-accessible Trp maximally emits above 350 nm and completely buried residue in hydrophobic environment emits near 320 nm, which means that Trp fluorescence maxima is dependent on the hydrophobicity of the surrounding environment. We observed that the wavelength of emission maxima of Trp residues in native CaLB was close to that of a buried Trp residue ~322 nm. The alteration of the microenvironment of the Trp residue(s) was supported by the decrease in fluorescence emission and accompanied by a red shift. The observed increase in λ_{max} might be due to movement of Trp residues to a more polar environment (Fig 5A). Fig 5B summarizes pH dependant changes in $FI_{322\ nm}$ and λ_{max} of

CaLB. A significant decline in FI $_{322\ nm}$ was noticed below pH 4.0 and above pH 9.0. As pH was lowered further the emission maxima began to increase, crossing a value of 339±0.76 nm at pH 2.6 and finally reached 346 nm at pH 12.0 with simultaneous decrease in FI. These observations suggest that the protein conformation under acidic conditions is different from native and 6 M GuHCl denatured state. The alkaline buffer show more significant effect on Trp microenvironment than the acidic ones. An apparent red shift of 25 nm (from 322±0.69 to 347±1.4 nm) of the Trp emission maxima from native condition (pH 7.4) was observed when the pH was > 10.5. In particular, Tyr residues in CaLB are likely to exist in the negatively-charged phenolate state due to ionization of the side chain hydroxyl moiety at pH > 10.5. Accordingly, changes in the ionization state of neighboring Tyr residues as the solution pH varies must also influence the intrinsic fluorescence of Trp residues in a highly subtle manner.

3.8. ANS binding

ANS is an extrinsic fluorescence probe which binds to loosely packed solvent accessible hydrophobic cores [31]. In the presence of a partially folded protein with exposed hydrophobic surfaces, the fluorescence of ANS is enhanced and the λ_{max} shifted from 510 nm (corresponding to free ANS) to ~480 nm (corresponding to protein bound ANS); consistent with the appearance of solvent-exposed hydrophobic surfaces (Fig 5C). In the present study, the λ_{max} of the ANS spectra in the presence of 6 M GuHCl, were at 513 nm (Table 3). The completely unfolded proteins do not bind to the probe, in spite of displaying a large amount of solvent-exposed hydrophobic surface [32].

As can be seen in the Fig 5D, insignificant change in ANS fluorescence intensity in the pH range 3.0-13.0 was observed. However with decrease in pH below 3.0, the ANS fluorescence intensity increases and was found to be maximum at pH 1.4, which thereafter decreases with blue shift. When ANS binds to exposed hydrophobic residues at pH 1.4,

ANS-FI was ~16 times more than native state, indicating enhanced exposure of hydrophobic patches. The partial unfolding leads the exposure of hydrophobic patches of proteins, which allows the interaction of ANS molecules and produces an enhanced ANS fluorescence as well as blue shifted emission maxima. This finding supports the CD data and also suggests that at low pH CaLB transforms to a partially unfolded intermediate state similar to that of molten globule-like state.

3.9. Acrylamide quenching studies

Quenching of Trp fluorescence by acrylamide is widely used to probe Trp environment in proteins. The extent of quenching by acrylamide was estimated by K_{sv} which were calculated by plotting linear Stern-Volmer plot between F_o/F and acrylamide concentration (Fig 6A) [33]. The K_{sv} value of native CaLB was found to be 1.97±0.01 M^{-1} while the corresponding values of K_{sv} at pH 2.6 and pH 1.4 were relatively higher, i.e. 2.15±0.03 and 2.67±0.03 M^{-1} respectively. However for the unfolded protein in 6 M GuHCl, the K_{sv} value is highest (3.64±0.04 M^{-1}). These result suggests that Trp residues of CaLB is less accessible to the quenchers in native condition while increased after Trp exposure in the MG state, which clearly indicates that the molten globule state is partially unfolded, exposing Trp residues for collisions with acrylamide. A comparison of the conformational properties of CaLB under pH 7.4, 2.6, 1.4 and 6 M GuHCl unfolded states are summarized in Table 3.

3.10. Dynamic light scattering (DLS) studies

DLS measures the hydrodynamic radii (R_h) and translational diffusion coefficient of a solute molecule in solution. The hydrodynamic radii (R_h) depend on the translational diffusion coefficient of a solute molecule and interparticle repulsive and attractive forces. The molecular topology of CaLB in solution was easily calculated by DLS experiments as a change of R_h and apparent molecular weight. As shown in Fig 6B and Table 4, R_h at pH

7.4, 2.6 and 1.4 were 27±0.01, 30±0.02 and 34±0.01 Å respectively. The CaLB under fully unfolded condition is characterized by progressive expansion in R_h ~41 Å (Fig 6B). The smallest R_h measured for native CaLB was 27±0.01 Å. At pH 2.6 and pH 1.4, as shown in the column diagram the column is higher at lower pH value. The changes in R_h are indicative of the acid-induced disruption of CaLB molecule and such increase in R_h value along with compact secondary structure, disrupted tertiary structure and exposed hydrophobic patches is characteristic feature of MG state. The pattern of MG state in CaLB is similar to the one reported for outer membrane protein from *Salmonella enteric* serovar Typhi [34]. Similar pattern was observed in apparent molecular weight for pH-induced unfolding of CaLB (Table 4). The progressive increase in the size of CaLB reflects the pH-induced unfolding reaction which well agrees with the hydrodynamic radii. While hydrodynamic radii and translational diffusion coefficient ($D_w^{25°C}$), describes the nature of molecules in solution phase, are inversely related to each other (equation no. 9). Therefore the values for $D_w^{25°C}$ followed opposite pattern with respect to R_h (Table 4). The result indicates that the effect of pH reflect some type of conformational changes upon lowering the pH favouring the self-association of CaLB. During DLS measurements, the polydispersity index (P_d) below 20%, suggests that the samples were in monodisperse phase, i.e., no aggregated species were present in the analyzed solutions (Table 4).

3.11. Size-exclusion chromatography

A calibration curve was generated by measuring the elution volumes (Ve), of 6 standard proteins whose Stokes radii are known in solution [24]. A standard plot for migration rate (1000/Ve) vs Stokes radius of each of standard proteins was plotted (Supplementary Fig S2). The data from the entire set of 6 standard proteins can be fit to a single linear equation:

$$\frac{1000}{\mathrm{Ve}} = 0.2944 R_{\mathrm{s}} + 9.2818 \quad (10)$$

The intermediate state of CaLB was determined by size-exclusion chromatography experiments. The elution profiles for CaLB at a representative set of different pH conditions are shown in Fig 6C. The protein shows a single, sharp peak after the elution procedure under defined conditions. The MG has an expanded dimension but retains substantial compactness. SEC show that the MG intermediate elutes earlier than protein at pH 7.4 and pH 2.6 unlike the species obtained in 6 M GuHCl which elutes earlier. The elution volume decreased from 58 to 50 ml when the pH was lowered from pH 7.4 to pH 1.4 (Fig 6C). CaLB show single peak corresponding to Stokes radii (R_s) and then increases linearly to a value of 27±0.02, 30±0.01, 36±0.02 and 51±0.04 Å, at pH 7.4, 2.6, 1.4 and 6 M GuHCl denatured state respectively (Fig 6D). Thus, the result indicate a slight increase in the hydrodynamic dimensions of the protein under acidic pH, which might be due to the opening up of the tertiary structure as compared to native state but they were found to be less than that of completely denatured state. The progressive increase in the size of CaLB reflects the pH-induced unfolding reaction which agrees well with the hydrodynamic radius. Further, R_h obtained from DLS and R_s from SEC are almost the same indication of loosening of the structure, characteristic feature of MG state (Table 4).

4. Guanidinium hydrochloride induced unfolding of CaLB

4.1. Changes in secondary structure as measured by circular dichroism

Far-UV CD spectra obtained under various GuHCl concentrations are shown in Supplementary Fig S3. The changes in the secondary structure of CaLB on increasing concentrations of GuHCl were reflected as marked changes in the shape and intensity of the spectra. However, up to 1.0 M GuHCl significant changes were observed only in the vicinity of 208 and 222 nm. Large changes around 222 nm regions were observed only after the addition of 2.0 M and higher GuHCl concentrations. The spectrum obtained at 5.0

M GuHCl resemble with 6.0 M GuHCl that of an extensively unfolded protein, and can be attributed largely to the strong chaotropic effect of GuHCl.

A comparison of MRE $_{222\ nm}$ values of different states (at pH 7.4, 2.6 and 1.4) with respect to varying GuHCl concentration show a significant change (Fig. 7A). The decrease in the MRE $_{222\ nm}$ reflects the disruption of secondary structure by increase in GuHCl. At native pH the unfolding transition curve continuously decreases up to 2.0 M and upon further increment in GuHCl molarity, no significant loss in secondary structure was observed. GuHCl induced unfolding of pH 2.6 show that CaLB stabilizes at low concentrations up to 0.5 M GuHCl and further increase in GuHCl concentration 0.5 M results in unfolding of CaLB [18]. Fig 7A (inset) shows the free energy change of unfolding (ΔG_u) as a function of GuHCl concentration, as calculated by equation no. 6. The experimental data can be fitted reasonably assuming two-state behavior of CaLB.

The concentration at midpoint of transition (C_m) was determined at the GuHCl concentration, where 50% of the protein was unfolded [35]. The C_m values were 1.08±0.03, 1.40±0.02 and 1.76±0.03 M at pH 7.4, 2.6 and 1.4 respectively. The extrapolated standard free energy changes, ΔG_u^o at zero GuHCl concentration were 7.72±0.29, 12.39±0.23 and 15.09±0.37 kcal mol^{-1} for pH 7.4, 2.6 and 1.4 respectively. The '*m*-value' is an important reaction coordinate which provides a measure of the solvent accessibility and consequently average compactness of intermediates. It is noteworthy that the '*m*-value' for the pH 7.4 is significantly smaller than that of pH 2.6 and pH 1.4 state of CaLB, as increase in '*m*-value' suggesting the disordering of CaLB at pH 2.6 and pH 1.4 (Table 5).

4.2. Changes in tertiary structure as measured by intrinsic fluorescence

The modification of the microenvironment of Trp residues of CaLB has been monitored by studying the changes in the emission intensity and wavelength maxima (λ_{max}). A comparative effect of increasing concentrations of GuHCl (0-6 M) on unfolding of CaLB

at pH 7.4, 2.6 and 1.4 was detected by intrinsic fluorescence measurements. We have recorded a series of fluorescence emission spectra at different GuHCl concentrations. The fluorescence intensity at 322 nm decreases with increasing GuHCl concentration, indicating the alteration in protein conformation. The sharp decrease in fluorescence between 1.0 M and 2.0 M GuHCl parallels the loss in helix content observed by CD (Fig 7B), indicating that the disruption of both secondary and tertiary structure occurs during this cooperative unfolding transition. Fluorescence intensity at pH 1.4 showed an initial increase until 0.75 M GuHCl and a decrease at 3.0 M and above. GuHCl below 0.75 M caused a minor red shift (~1 nm), whereas major structural changes were induced only at 4 M and reached a plateau at 6 M GuHCl concentration. The inset of Fig 7B shows typical linear extrapolation analysis at 25 °C to evaluate the folding free energy, ΔG_u^o and '*m*-values' respectively from the intercept and the slope of the plot of the free energy of unfolding at different denaturant concentrations (equation no. 6). The ΔG_u^o for native and MG state are 12.26±0.61 and 17.08±0.82 kcal mol^{-1} (Table 5). At pH 7.4, 2.6 and 1.4, the C_m values were 0.56±0.03, 1.35±0.02 and 1.51±0.01 M respectively. Fig 7B (inset) and Table 5 shows the '*m*-values' obtained were very different at pHs: 7.4, 2.6 and 1.4 (21.89±1.08, 11.65±0.83 and 11.3±0.02 kcal mol^{-1} M^{-1} respectively) which suggests that the different states are involved in the unfolding transition in this pH interval. The unfolded conformation of the protein display greater exposure to the solvent than neutral pH. Thus, the decrease in pH in presence of the chemical denaturant has a drastic effect on the stability of the protein.

4.3. Equilibrium unfolding studies by extrinsic fluorescence spectroscopy using ANS as an external fluorophore

For the further insight of structural properties of CaLB, we investigated the binding of ANS at pH 7.4, 2.6 and 1.4 in presence of increasing concentration of GuHCl. Change in

FI value at 480 nm implies that the observed increase in ANS binding fluorescence on addition of low concentration of GuHCl is due to more exposed hydrophobic surface than that of the high concentration of GuHCl. At pH 7.4, there was no significant differential ANS binding capacity of CaLB denatured with GuHCl as compared to the pH 2.6 and pH 1.4 state (Fig 7C). At pH 2.6, gradual increase in ANS emission intensity at 0.5 M GuHCl concentration is usually interpreted as indicative of a greater solvent accessibility of the protein interior and the formation of an intermediate conformational state. Furthermore, the drop of fluorescence intensity of ANS at high concentrations of GuHCl is interpreted as complete protein denaturation. Thus, it is clear that GuHCl-treated CaLB possesses different measures of exposed hydrophobic areas in the presence of different concentrations of GuHCl. These values are similar to those obtained by following the changes in the intrinsic fluorescence. The decrease in emission maxima and intensity is suggestive of internalization of exposed Trp residues within the molecule which in turn increases its proximity with specific quenching groups.

Refolding of CaLB denatured from GuHCl followed by fluorescence spectroscopy

Kinetic curves of CaLB unfolding and refolding from the native (0 M GuHCl) and unfolded state (4 M GuHCl), which were monitored by intrinsic tryptophan fluorescence at various GuHCl concentrations. To compare the refolding effects of GuHCl, we performed similar experiments as reported in previous studies [19, 36, 37], the refolding of GuHCl denatured CaLB was initiated by dilution (Fig 8). A representative kinetic trace for refolding of CaLB at a final GuHCl concentration of 1.0 M, after the burst phase, was analyzed by fitting to double exponential equation 8 and the results are summarized in Table 6. The emission intensity increases dramatically in the burst phase to an amplitude of ~11 times that of the native enzyme at a final GuHCl concentration of 1.0 M. The intrinsic fluorescence of the rapidly formed intermediate is even greater than that of the

stable equilibrium intermediate and significant increase in fluorescence intensity which was stabilized within ~100 seconds. Refolding occurs in two kinetic phases, one fast and one slow (Fig 8). To further elucidate the rate constant k_{fast} and k_{slow} were 1.32 s^{-1} and 4 s^{-1} respectively, at a final GuHCl concentration 1.0 M, which is consistent with those reported in previous studies. The extent of fluorescence intensity was considerably reduced when GuHCl concentration of 2.0 M. The rate constant obtained in presence of 2.0 M GuHCl concentration rate constant were k_{fast} 0.93 s^{-1} and k_{slow} 2.78 s^{-1} which shows that GuHCl affects the rapid phase of CaLB. The refolding curves for CaLB at final (4.0 M) GuHCl concentrations, rate constant were k_{fast} 0.68 s^{-1} and k_{slow} 2.08 s^{-1} respectively. The rate constants for both the fast and slow phases decrease with increase in GuHCl concentration upto 4.0 M .

5. Thermal Stability of CaLB

5.2. Thermal stability measurement by differential scanning calorimetry

The thermal stability of CaLB has been evaluated by DSC measurements in a pH range of 1.0-13.0. The DSC profile at pH 7.4, pH 2.6 and pH 1.4 are presented in Fig 9A. The heat capacity at constant pressure (C_p) produced a wide endotherm, suggesting a two-state transition with a temperature midpoint (T_m) of 57.9±0.01 °C for CaLB at pH 7.4 (Table 7). At pH 2.6, the small heat signal suggests that CaLB is likely to have undergone structural changes during the thermal unfolding recorded by the DSC with a temperature midpoint (T_m) 54.1±0.02 °C. At pH 1.4 and below, no thermal transition could be obtained by DSC it may be because of unordered tertiary structure of CaLB (Fig 9A). The DSC profile of CaLB was fitted using a non-two-state model to calculate the calorimetric heat change (ΔH_{cal}) and van't Hoff heat change (ΔH_{vH}) ratio. At pH 7.4, the calorimetric enthalpy (ΔH_{cal}) estimated directly from the DSC curve is 101±0.38 kcal mol^{-1}, which is close to the van't Hoff enthalpy (ΔH_{vH}) (104±0.49 kcal mol^{-1}). If $\Delta H_{vH} = \Delta H_{cal}$ then the denaturation

can be considered to be well approximated by a two state unfolding process. Denaturation enthalpy change around 204 kcal mol^{-1} at 60 ºC for a protein of 305 amino acids, according to Robertson and Murphy [38]. The thermal unfolding is an irreversible process, as cooling and immediate reheating of CaLB does not generate a DSC peak. The observation is attributed to aggregation phenomena which are related to thermal unfolding of proteins. The denaturation process accurately explained by two-state irreversible model [39, 40].

Overall, the data suggested that the unfolding of CaLB in acid conditions proceeded through a two state mechanism. The thermal unfolding is an irreversible process, as cooling and immediate reheating of CaLB do not generate sharp DSC peak. Calorimetric data analysis showed an enthalpy value slightly smaller at 2.6 than in pH 7.4. As expected, the acid unfolded MG state (pH 1.4), show no thermal transition by DSC it may be due to unordered tertiary structure of CaLB as proved by far, near-UV CD, tryptophan fluorescence, ANS-FI and SEC experiments. Since loss in heat capacity (C_p) is related to the molecular interactions that maintain tertiary and secondary structure of CaLB, this result suggests that CaLB was suffering through the unfolding process by pH.

5.1. Thermal stability measurement by far-UV CD

Thermal denaturation of CaLB at pH 7.4 and 2.6 as studied by far-UV CD seems to be a two state process. The secondary structure of CaLB at pH 7.4 and pH 2.6 remained intact at temperature up to 50 °C, further increase in temperature cause gradual decrease in $MRE_{222\ nm}$. At pH 7.4 and 2.6 the curve shows a single-phase transition with estimated T_m of 57±0.8 and 53±0.6 °C respectively. While at pH 1.4, CaLB was unstable and follow noncooperative path, as expected for molten globule state (as monitored by far-UV CD spectroscopy). This evidence supports the existence of rigid and compact structure at pH 2.6, with strong intra-molecular interactions between the side chains of constituent amino acids. Evidently, the MG state of CaLB is considerably less stable than the native state

showed complete distortion in secondary structure, judged by decrease in the negative ellipticity (Fig 9B). From Fig 9A and B, it is clear that as pH decreases, the transition broadened and the denaturation temperature (T_m) increases. These results indicate that with the change in pH, CaLB undergoes subtle conformational changes. During these conformational changes, only the number of hydrogen bonds increases apparently without any change in intramolecular nonpolar groups. Reversibility of the thermal unfolding was confirmed by heating up to 95 °C, thermally unfolded sample was cooled down to 25 °C at a rate of 1 °C min^{-1} and then re-heated to 95 °C while recording the molar ellipticity at 222 nm. Further heating of CaLB sample do not follow the sigmoid pattern, so this experiment proves that CaLB is thermally unstable protein. The native state of (pH 7.4) CaLB has free energy (ΔG_u^o) of 10.5±0.5 kcal mol^{-1}, whereas at pH 2.6 has ΔG_u^o 19.9±0.2 kcal mol^{-1} (Table 7). These results suggest that more ordered and stable secondary structure exist at pH 7.4 while at pH 1.4, CaLB becomes more disordered and thermally less stable. Therefore this is considered as the classical acid induced molten globule state of CaLB exists at pH 1.4.

6. Discussion

Structural studies and unfolding transitions of proteins under different solvent conditions provide information about the conformation of protein molecules and the role of various stabilizing and destabilizing forces responsible for the unique three-dimensional structure of proteins [41]. It has been demonstrated that the ability to keep the protein in native and functional structure over a particular range of temperatures, pH levels, and salinities is an intrinsic property of the protein molecule itself, outside this range, the molecule starts losing its secondary and tertiary structure [42].

Candida antarctica lipase B (CaLB) is the most widely studied cold adapted lipase with a great number of registered patents and various applications, which encourage utilization of the enzyme as an appropriate candidate in pharmaceutical, chemical and food industries. [43]. Spectroscopic, calorimetric and chromatographic techniques were employed in this study to characterize different states populated at varying pHs. More importantly, our spectroscopic studies revealed that the surface of CaLB is heavily decorated with ionizable residues such as Asp, Glu and His. Accordingly, these ionizable residues must play a key role in the acid-induced association of CaLB into a molten globule state as observed here. Thus, under acidic conditions, protonation will result in the neutralization of negative charge on Asp/Glu residues, while His residues will gain a net positive charge. Such change in electrostatic polarity may not only promote association of CaLB into a molten globule state observed here but would also likely render it thermodynamically more favorable for the protein to facilitate the formation of a molten globule required. It is also conceivable that one or more His residues may engage in some sort of ion pairing with Asp/Glu residues at neutral pH, where His will be positively charged but Asp/Glu will bear a net negative charge, in an intramolecular manner. However, as the pH becomes more acidic, the neutralization of negative charge on Asp/Glu residues will disfavor such intramolecular ion pairing with His and may facilitate the formation of intermediate state as observed at pH 2.6 and pH 1.4. Importantly, such a scenario is plausible in light of our structural models.

Extreme acidic pH unfolds proteins by affecting the electrostatic interactions. Acid-induced unfolding of proteins is often incomplete and it assumes the conformations that are located between native and completely unfolded state [44, 45]. The major driving force involved during acid denaturation is an intra-molecular charge repulsion, which may or may not overcome the interactions favoring the folded states such as hydrophobic forces,

salt bridges and metal ion-protein interactions in case of metalloproteins [46]. The mechanism of denaturation of a given protein at low pH is proposed to be complex and may involve intricate interplay between a variety of stabilizing and destabilizing forces leading to a relatively compact structure, characteristic of the molten globule or partially unfolded intermediate [47].

The present study demonstrates that CaLB exists as a partially unfolded state at acidic pH with the characteristic features of molten globule. The observed structural properties of CaLB at pH 1.4 agrees with the definition of the molten globule state as it contains disordered tertiary structure but retains 67% secondary structure with strong ANS binding. The protein molecule in the molten globule state can effectively interact with the hydrophobic fluorescent probe i.e. ANS [48], because of the accessible hydrophobic solvent. It is characterized by a considerable secondary structure, although much less pronounced than that of the native or the molten globule protein (protein in the pre-molten globule state has ~50% of the native secondary structure, whereas in the molten globule state the corresponding value is noticeably higher). The protein molecule in the molten globule state is considerably less compact than in the native states, but it is still more compact than the random coil. The loss of native side-chain packing is expected to render a MG state functionally inactive. A comparison of some of the conformational properties of CaLB under native, molten globule and unfolded states are summarized in Table 1.

The GuHCl denaturation of CaLB at pH 7.4, 2.6 and 1.4 further confirms the possibility that at low concentration the stabilizing action of GuHCl dominates over denaturing effect. Due to this, the stability difference between the two structural entities decreases and they unfold as a single entity at higher concentration of denaturant leads to cooperative transition by various probes. The stabilization action of GuHCl originates from its ionic nature and its role in stabilization of protein may involve both entropic effect and ionic

interactions. The entropic effect is due to the cross-linking action of GuH^+ cations by forming hydrogen bonds and van der Waals interactions with different nonspecific parts of the protein while the electrostatic effect arises due to the interaction of Cl^-, and also of GuH^+ with charged groups of the protein. The '*m*-values' appears to decrease slightly with decrease in pH, suggesting that the variation in '*m*-values' is believed to be due to change in the solvent-accessible area of hydrophobic residues. The '*m*-values' are higher in the case of pH 7.4 than the pH 2.6 and pH 1.4 (Table 5), which means the thermal transition of CaLB is less cooperative at pH 2.6 and pH 1.4.

In this respect, it is noteworthy that our CD spectra revealed the maintenance of CaLB's regular secondary structure and partial loss of tertiary structure at pH 2.6, in contrast to the complete loss of tertiary structure observed at pH 1.4. A considerable decrease in the unfolding transition temperature and loss of unfolding cooperativity was observed at pH 2.6, but complete loss occured at pH 1.4. The dramatic enhancement of ANS fluorescence intensity is evident upon binding by CaLB at pH 2.6 and 1.4. Thus, all the experimental data are consistent with the existence of an MG-like state at low pH.

The refolding process of CaLB is characterized by the presence of a burst phase intermediate with significant tertiary structural elements. A considerable blue shift in λ_{max} emission of tryptophan fluorescence was observed in the burst phase intermediate upon refolding (350 nm for unfolded protein to 325 nm for burst phase intermediate, data not shown). It suggests the collapse of the unfolded CaLB to compact state (C state) leading to burial of most of the tryptophan residues in the latter. A fast pre-equilibrium can be assumed for the U $\leftrightarrow$ C transition during early stage of CaLB refolding. Although the C state consists of some non-native secondary structure, a significant native secondary structure is also present in it (Table 1). These observations are consistent with the existing folding model which reveals that both local and nonlocal interactions are dominant forces

in early folding intermediates. Such intermediates having a compact collapsed structure, stabilized by hydrophobic interactions and local hydrogen bonds, are useful for guiding the folding process of large proteins, as it would become increasingly difficult to form specific nonlocal interactions unless the molecule assumes the compact conformation.

We have detected MG state which is conformationally different from native CaLB. Moreover, the gradual increase in hydrodynamic radii and Stokes radii of the CaLB with decreasing in pH suggests an unfolding process, the magnitude of this change (from 27 Å for native to 34 Å for MG state of CaLB) being sufficient to account for any appreciable extension or unfolding of the CaLB molecule. Protein disorder also manifests itself in other physical characteristics, such as aberrant mobility in gel filtration. As a consequence of their unique amino acid composition and highly hydrophilic nature, their hydrodynamic radii are usually much larger than that of a globular protein of the same size, causing them to elute at a much higher apparent molecular weight than expected. The difference between the apparent and the real molecular weight of a specific disordered protein depends on its amino acid sequence and exact hydrodynamic behavior [49]. Additionally, our chemical denaturation studies for both native and low pH-forms support that the conformational isomer formed at pH 1.4 is less thermodynamically stable than the native protein.

The findings of this study suggest that psychrophilic nature of CaLB might be a result of a delicate combination of different factors, which simultaneously play role to stabilize the CaLB at low temperature. Not simply amino acid sequence, but also surface hydrophobic clusters are deciding factor, that enables the protein to have an optimized dynamic feature according to its functional temperature [50]. Flexibility of CaLB at low pH is localized to its active site, while the global stability of enzyme is not significantly affected by pH. The three disulfide bonds help in providing the stability of enzyme from being denatured at both low and high pH. Ganjalikhany et al documented that modulation of α5 followed by

change in the orientation of the side chains just before the cleft results in the closed conformation where a component of active site is guarded by conformational relocation. The dual factors are playing role in the enzymatic activation, one is the closed conformation while other is enhanced flexibility of loop involving amino acid residues from 183-208 as confirmed by essential dynamics analysis at 35 and 50 °C to validate the thermo sensitivity of CaLB. Considering that the loop is holding catalytic residue (Asp 187), increase in the flexibility of this region would probably disarrange the geometry of catalytic triad [51]. At pH lower than 5.0, CaLB is positively charged while from pH 5.0 to 9.0, CaLB is neutral. Due to the lack of titratable groups in this pH range, the change in protonation is almost negligible. As the active site of CaLB shares the common catalytic triad Ser105-Asp187-His224, the active site being only a small part of the whole enzyme molecule, thus, its unfolding at a certain pH condition results loss of enzymatic activity. The finding of this study, the lipases has ‘‘catalytic triad,’’ which setup an H^+ shuttle or the charge relay system at the active site of lipase that affects the activity and specific activity of the lipase catalyzed reactions.

7. Conclusion

The present work describes the identification and characterization of pH-dependent conformational intermediates of CaLB using fluorescence measurements of extrinsic and intrinsic probes. We found that intermediate exists over pH denaturation of CaLB induced by low pH and intermediate populated at pH 1.4 is characterized as molten globule state with stable secondary structure, disrupted tertiary structure, exposed hydrophobic surface and enhanced ANS binding. However, there is increasing evidence that molten globules are common and play a key role in a wide variety of physiological processes, including translocation across membranes, increased affinity for membranes, binding to liposome and phospholipids, protein trafficking, extracellular secretion, and the control and

regulation of the cell cycle [34]. Our finding is relevant in the context of the observation that partially-destabilized proteins comprising exposed hydrophobic regions are prone to aggregate formation which might have important implications in protein misfolding and aggregation-related disorders.

Acknowledgements

G. Rabbani, acknowledged to Council of Scientific and Industrial Research (CSIR), New Delhi, India for financial assistance in the form of Senior Research Fellow (SRF). This work was supported by the CSIR funded project, New Delhi, Govt. of India grant No. 37(1456)/10/EMR-II. The authors are highly thankful to Dr. Piers Gatenby (University College London) for his suggestions, thorough editing and proofreading of the manuscript.

References

1 G. Feller and C. Gerday, *Nat Rev Microbiol*, 2003, **1**, 200-208.
2 C. Gerday, M. Aittaleb, M. Bentahir, J. P. Chessa, P. Claverie, T. Collins, S. D'Amico, J. Dumont, G. Garsoux, D. Georlette, A. Hoyoux, T. Lonhienne, M. A. Meuwis and G. Feller, *Trends Biotechnol*, 2000, **18**, 103-107.
3 R. Margesin and G. Feller, *Environ Technol*, 2010, **31**, 835-844.
4 J. C. Marx, T. Collins, S. D'Amico, G. Feller and C. Gerday, *Mar Biotechnol (NY)*, 2007, **9**, 293-304.
5 S. D'Amico, T. Collins, J. C. Marx, G. Feller and C. Gerday, *EMBO Rep*, 2006, **7**, 385-389.
6 J. C. Marx, V. Blaise, T. Collins, S. D'Amico, D. Delille, E. Gratia, A. Hoyoux, A. L. Huston, G. Sonan, G. Feller and C. Gerday, *Cell Mol Biol (Noisy-le-grand)*, 2004, **50**, 643-655.
7 G. Feller, *Extremophiles*, 2007, **11**, 211-216.
8 A. L. Huston, J. Z. Haeggstrom and G. Feller, *Biochim Biophys Acta*, 2008, **1784**, 1865-1872.
9 A. E. Fedoy, N. Yang, A. Martinez, H. K. Leiros and I. H. Steen, *J Mol Biol*, 2007, **372**, 130-149.
10 J. L. Adrio and A. L. Demain, *Biomolecules*, 2014, **4**, 117-139.
11 M. Lazniewski, K. Steczkiewicz, L. Knizewski, I. Wawer and K. Ginalski, *FEBS Lett*, 2011, **585**, 870-874.
12 M. Irani, U. Tornvall, S. Genheden, M. W. Larsen, R. Hatti-Kaul and U. Ryde, *Biochemistry*, 2013, **52**, 1280-1289.
13 Q. Wu, P. Soni and M. T. Reetz, *J Am Chem Soc*, 2013, **135**, 1872-1881.
14 S. Fatima, B. Ahmad and R. H. Khan, *IUBMB Life*, 2007, **59**, 179-186.
15 A. Idris and A. Bukhari, *Biotechnol Adv*, 2012, **30**, 550-563.
16 D. P. Kumar, A. Tiwari and R. Bhat, *J Biol Chem*, 2004, **279**, 32093-32099.
17 S. Nakamura, Y. Seki, E. Katoh and S. Kidokoro, *Biochemistry*, 2011, **50**, 3116-3126.
18 G. Rabbani, E. Ahmad, N. Zaidi, S. Fatima and R. H. Khan, *Cell Biochem Biophys*, 2012, **62**, 487-499.
19 A. Maheshwari, V. K. Verma and T. K. Chaudhuri, *Biochimie*, 2010, **92**, 491-498.
20 M. H. Gangadhariah, B. Wang, M. Linetsky, C. Henning, R. Spanneberg, M. A.

Glomb and R. H. Nagaraj, *Biochim Biophys Acta*, 2010, **1802**, 432-441.
21 S. C. Gill and P. H. von Hippel, *Anal Biochem*, 1989, **182**, 319-326.
22 Y. H. Chen, J. T. Yang and H. M. Martinez, *Biochemistry*, 1972, **11**, 4120-4131.
23 C. N. Pace and K. L. Shaw, *Proteins*, 2000, **Suppl 4**, 1-7.
24 V. N. Uversky, *Biochemistry*, 1993, **32**, 13288-13298.
25 J. Uppenberg, S. Patkar, T. Bergfors and T. A. Jones, *J Mol Biol*, 1994, **235**, 790-792.
26 S. M. Kelly, T. J. Jess and N. C. Price, *Biochim Biophys Acta*, 2005, **1751**, 119-139.
27 O. B. Ptitsyn, *Adv Protein Chem*, 1995, **47**, 83-229.
28 P. Trodler, J. Nieveler, M. Rusnak, R. D. Schmid and J. Pleiss, *J Chromatogr A*, 2008, **1179**, 161-167.
29 R. B. Cundall, A.Keith Davies, Peter G. Morris and J. Williams, *J Photochemistry*, 1981, **17**, 369-376.
30 V. Fodera, M. Groenning, V. Vetri, F. Librizzi, S. Spagnolo, C. Cornett, L. Olsen, M. van de Weert and M. Leone, *J Phys Chem B*, 2008, **112**, 15174-15181.
31 M. R. Eftink, *Biophys J*, 1994, **66**, 482-501.
32 A. Varshney, B. Ahmad, G. Rabbani, V. Kumar, S. Yadav and R. H. Khan, *Amino Acids*, 2010, **39**, 899-910.
33 M. R. Eftink and C. A. Ghiron, *Biochim Biophys Acta*, 1987, **916**, 343-349.
34 G. Rabbani, J. Kaur, E. Ahmad, R. H. Khan and S. K. Jain, *Appl Microbiol Biotechnol*, 2014, **98**, 2533-2543.
35 G. J. He, A. Zhang, W. F. Liu, Y. Cheng and Y. B. Yan, *FEBS J*, 2009, **276**, 2849-2860.
36 V. Dahiya and T. K. Chaudhuri, *Biochemistry*, 2013, **52**, 4517-4530.
37 M. Suzuki, K. Yokoyama, Y. H. Lee and Y. Goto, *Biochemistry*, 2011, **50**, 10390-10398.
38 A. D. Robertson and K. P. Murphy, *Chem Rev*, 1997, **97**, 1251-1268.
39 J. M. Sanchez-Ruiz, *Biophys J*, 1992, **61**, 921-935.
40 D. Rodriguez-Larrea, S. Minning, T. V. Borchert and J. M. Sanchez-Ruiz, *J Mol Biol*, 2006, **360**, 715-724.
41 P. K. Devaraneni, N. Mishra and R. Bhat, *Biochimie*, 2012, **94**, 947-952.
42 C. B. Anfinsen, *Science*, 1973, **181**, 223-230.
43 B. Joseph, P. W. Ramteke and G. Thomas, *Biotechnol Adv*, 2008, **26**, 457-470.
44 G. Rabbani, E. Ahmad, N. Zaidi and R. H. Khan, *Cell Biochem Biophys*, 2011, **61**, 551-560.
45 T. Rasmussen, M. van de Weert, W. Jiskoot and M. R. Kasimova, *Proteins*, 2011, **79**, 1747-1758.
46 A. Sujak, N. J. Sanghamitra, O. Maneg, B. Ludwig and S. Mazumdar, *Biophys J*, 2007, **93**, 2845-2851.
47 M. Z. Kamal, S. Ahmad, T. R. Molugu, A. Vijayalakshmi, M. V. Deshmukh, R. Sankaranarayanan and N. M. Rao, *J Mol Biol*, 2011, **413**, 726-741.
48 V. N. Uversky and O. B. Ptitsyn, *Biochemistry*, 1994, **33**, 2782-2791.
49 A. Tantos, K. Szrnka, B. Szabo, M. Bokor, P. Kamasa, P. Matus, A. Bekesi, K. Tompa, K. H. Han and P. Tompa, *Biochim Biophys Acta*, 2013, **1834**, 342-350.
50 D. Georlette, B. Damien, V. Blaise, E. Depiereux, V. N. Uversky, C. Gerday and G. Feller, *J Biol Chem*, 2003, **278**, 37015-37023.
51 M. R. Ganjalikhany, B. Ranjbar, A. H. Taghavi and T. Tohidi Moghadam, *PLoS One*, 2012, **7**, e40327.

Legends to figures

Fig. 1 Cartoon representation of CaLB (cyan) from PDB ID: 1LBS [Uppenberg et al., 1994] with all the five Trp residues (red), two N-Acetyl-D-glucosamine molecules (purple) and one N-hexylphosphonate ethyl ester (green).

Fig. 2 (A) Far-UV CD spectra of CaLB at pH 7.4, 2.6, 1.4 and 6 M GuHCl denatured state respectively. To check the reversibility of CaLB samples were incubated at pH 1.0 and 11.0, further to refold the native state the pH of sample is re-adjusted to pH 1.0 → 7.4 and pH 11.0 → 7.4. **(B)** Effect of pH on MRE $_{222}$ nm of CaLB at different pH (-○-) and 6 M GuHCl (●).

Fig. 3 (A) Near-UV CD spectra of CaLB at pH 7.4, 2.6, 1.4 and 6 M GuHCl denatured state respectively. Reversibility of CaLB samples were incubated at pH 1.0 and 11.0, further allowed refolding the native state the pH of sample is re-adjusted to pH 1.0 → 7.4 and pH 11.0 → 7.4. **(B)** Effect of pH on MRE $_{277}$ nm of CaLB at different pH (-○-) and 6 M GuHCl (●).

Fig.4 (A) Turbidity measurements of CaLB carried out by taking absorbance at 350 nm. **(B)** Rayleigh scattering of CaLB measured at 350 nm, samples were excited at 350 nm. ThT fluorescence intensity at 480 nm of CaLB from pH 1.0 to 13.0.

Fig. 5 (A) Intrinsic fluorescence spectra of CaLB at pH 7.4, 2.6, 1.4 and 6 M GuHCl denatured respectively. **(B)** Change in intrinsic fluorescence intensity at 322 nm *vs* λ_{max} of CaLB. **(C)** ANS binding to CaLB at pH 7.4, 2.6, 1.4 and 6 M GuHCl denatured respectively (captions are same as in fig. 4A). **(D)** Change in extrinsic fluorescence intensity at 480 nm of CaLB at different pH (-○-) and 6 M GuHCl (●).

Fig. 6 (A) Stern-Volmer plots for acrylamide quenching of Trp fluorescence of CaLB. **(B)** Measurement of hydrodynamic radii of CaLB at different pH (pH 7.4, 2.6 and 1.4) and 6 M GuHCl denatured. **(C)** Elution profiles of CaLB at different pH (pH 7.4, 2.6 and 1.4) and 6 M GuHCl denatured state. **(D)** Linear fit of Stokes radii vs 1000/Ve of CaLB at different pH (pH 7.4, 2.6 and 1.4) and 6 M GuHCl denatured state.

Fig. 7 (A) GuHCl-induced unfolding of CALB at pH 7.4, 2.6 and 1.4. Unfolding transition monitored by MRE at 222 nm and free energy plot for stability (inset). **(B)** GuHCl-induced unfolding of CALB at pH 7.4, 2.6 and 1.4. Unfolding transition monitored by intrinsic fluorescence at 322 nm and free energy plot for tertiary structure stability (inset). **(C)** Extrinsic fluorescence at 480 nm for CALB at pH 7.4, 2.6 and 1.4 at varying GuHCl concentrations.

Fig. 8 Effect of GuHCl concentration on the refolding kinetics of CaLB. The refolding kinetics of CaLB was monitored by change in tryptophan fluorescence at 322 nm in sodium phosphate buffer pH 7.4, 25 °C. Protein was excited at 280 nm. Refolding kinetic traces (colored line) when protein unfolded in 1.0, 2.0 and 4.0 M GuHCl concentration and CaLB further refolded by diluting GuHCl in the refolding buffer (top to bottom). The continuous black lines are the least-square fits of data to double exponential equation.

Fig. 9 (A) Calorimetric melting profile of CaLB: at 10 μM, at pH 7.4, pH 2.6 and 1.4 in 20 mM sodium phosphate buffer at pH 7.4, Glycine-HCl pH 2.6 and KCl-HCl pH 1.4. The obtained thermodynamic parameters are summarized in table 7. **(B)** Thermal unfolding of CaLB as followed by CD spectroscopy at 222 nm; the heating rate was 1 °C min^{-1}. Measurements were carried out using a protein concentration of 6 μM and in same above buffers.

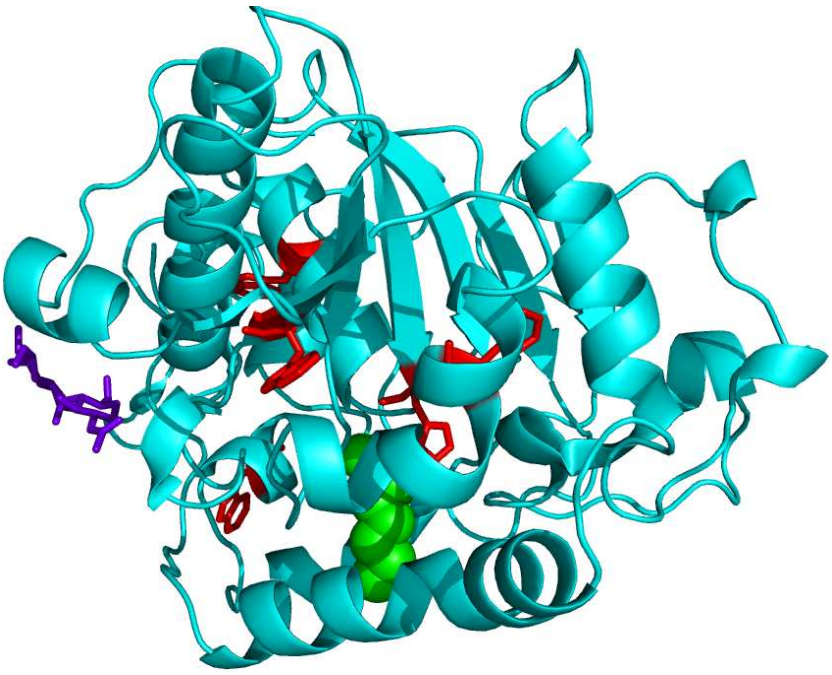

Fig. 1

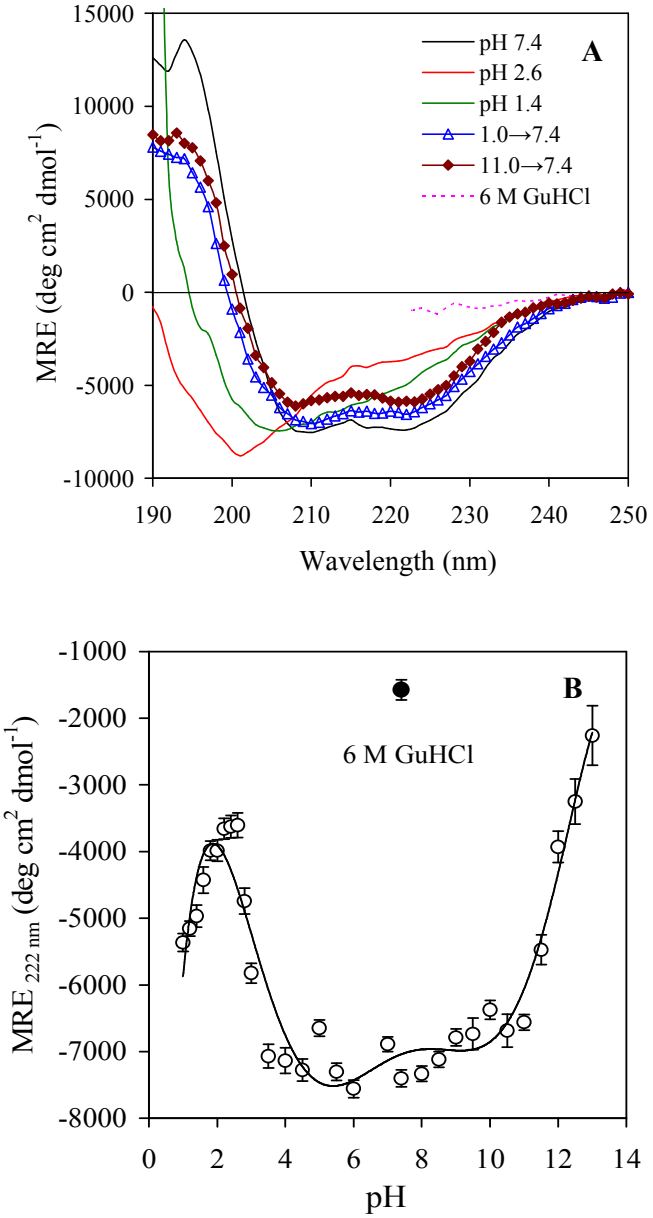

Fig. 2

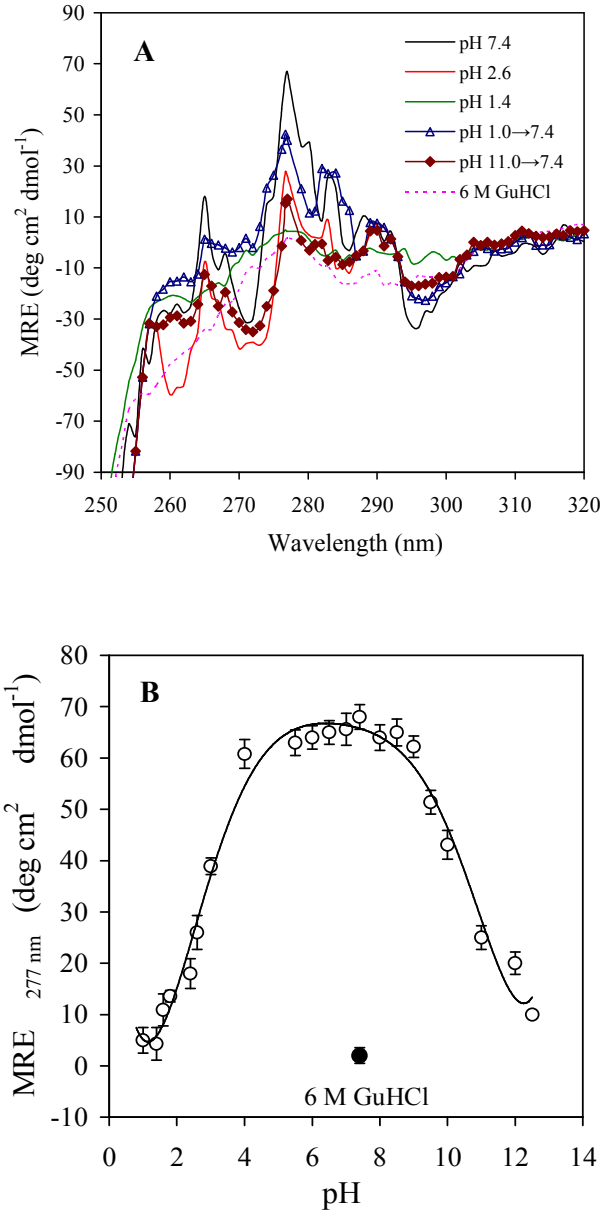

Fig. 3

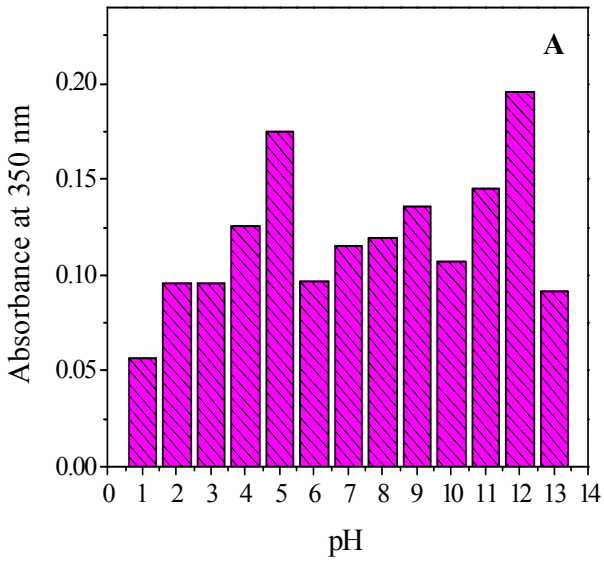

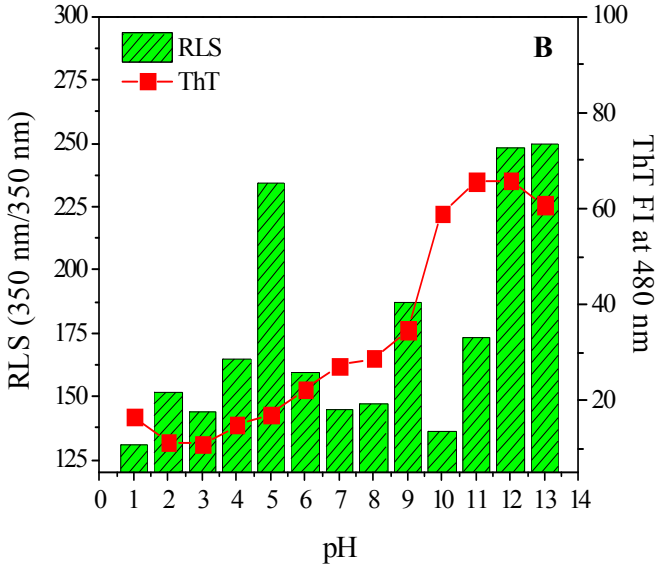

Fig. 4

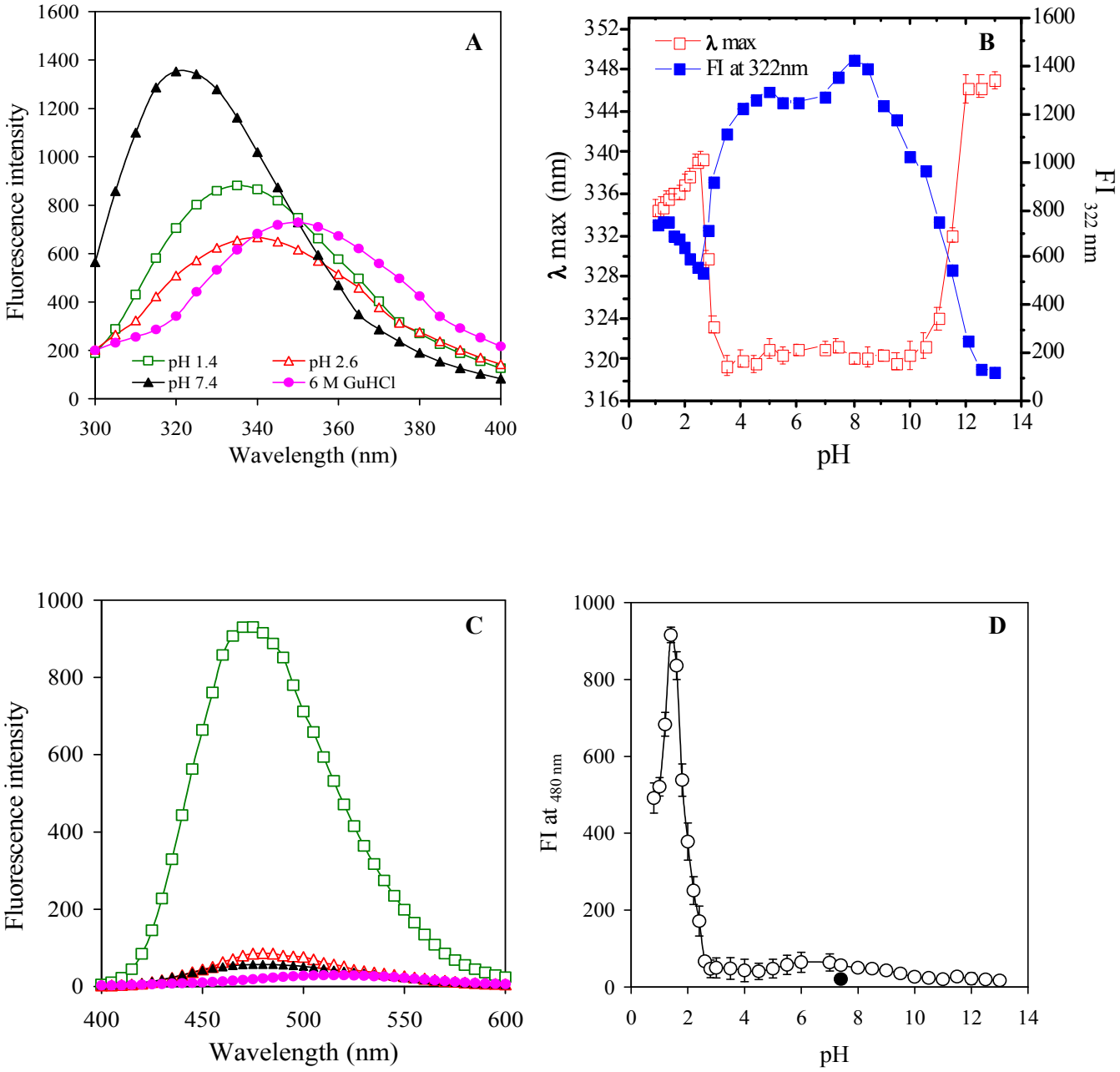

Fig. 5

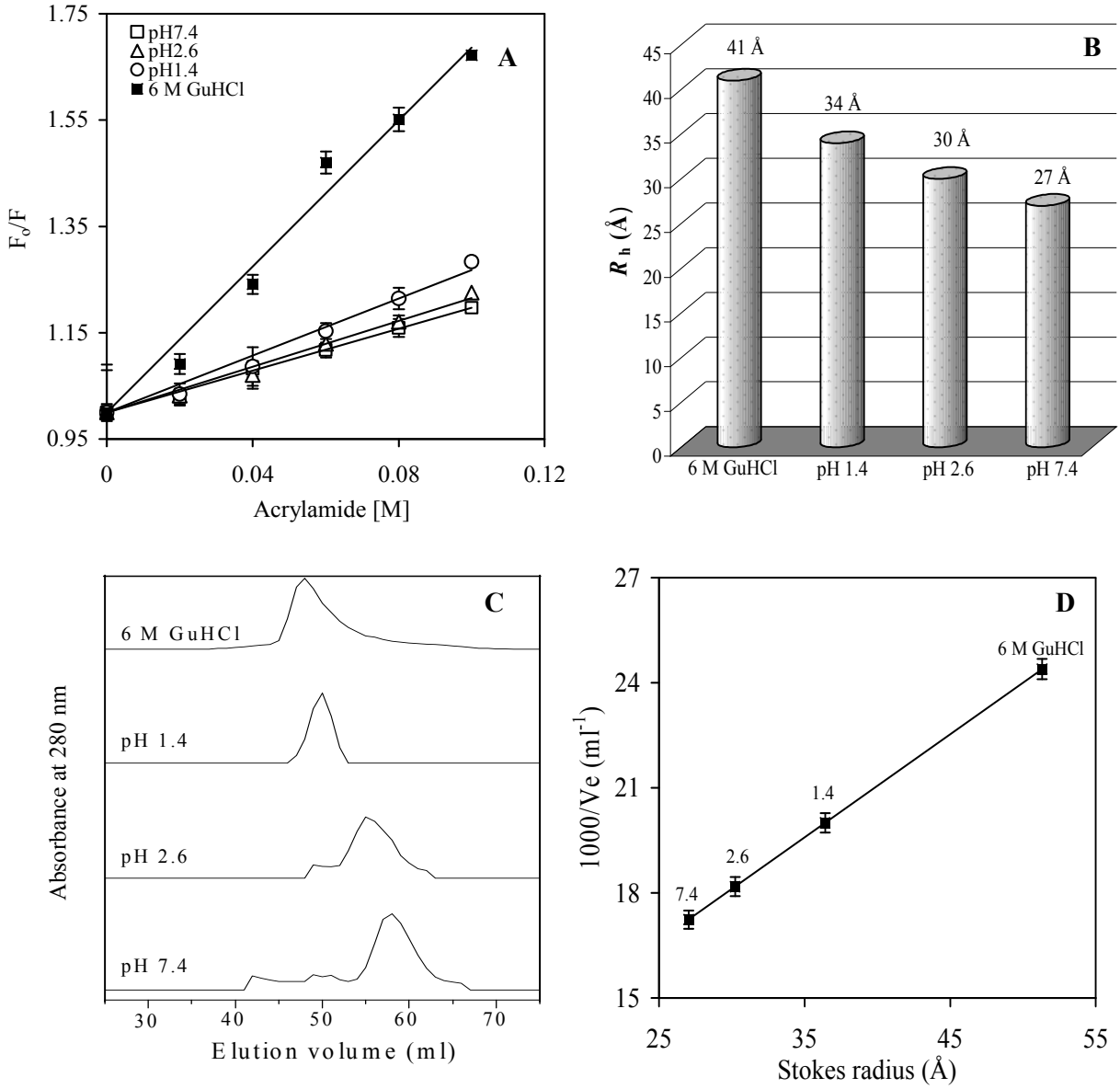

Fig. 6

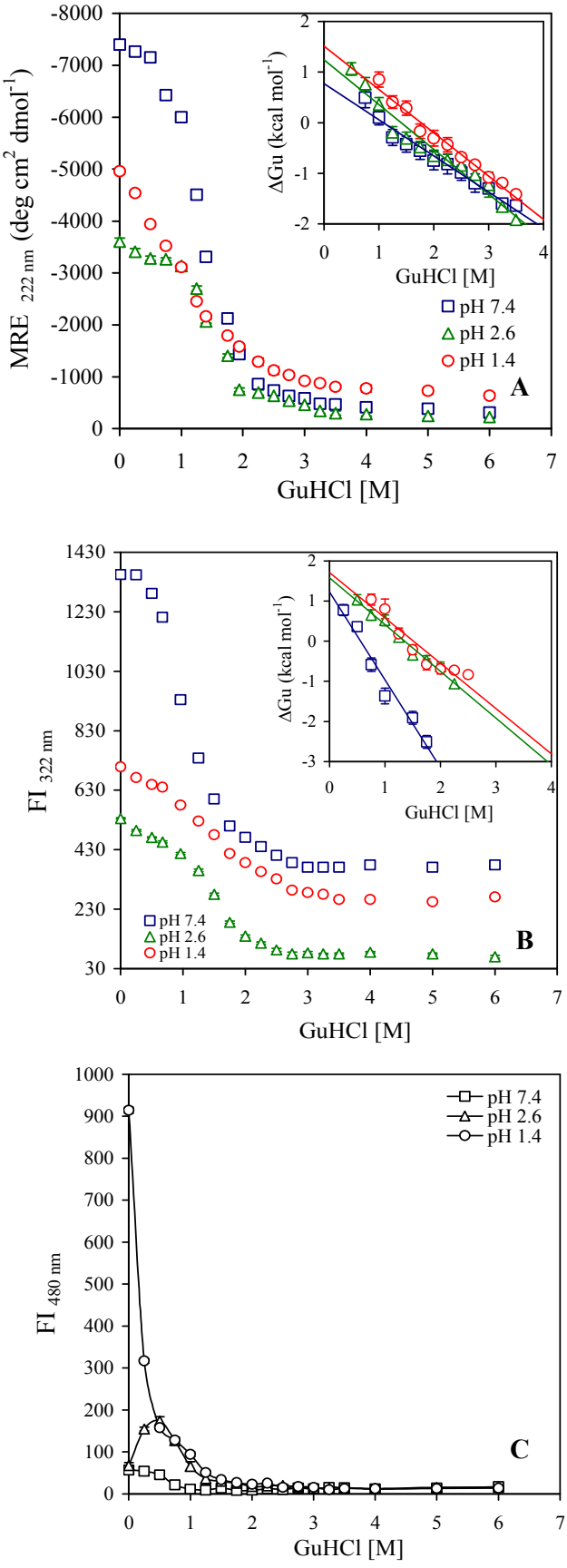

Fig. 7

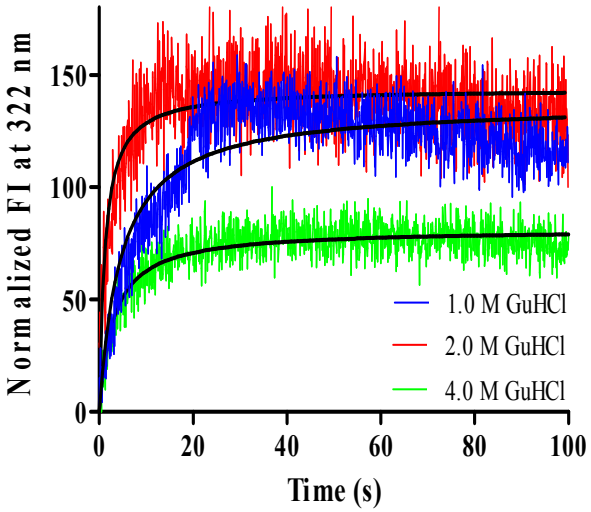

Fig. 8

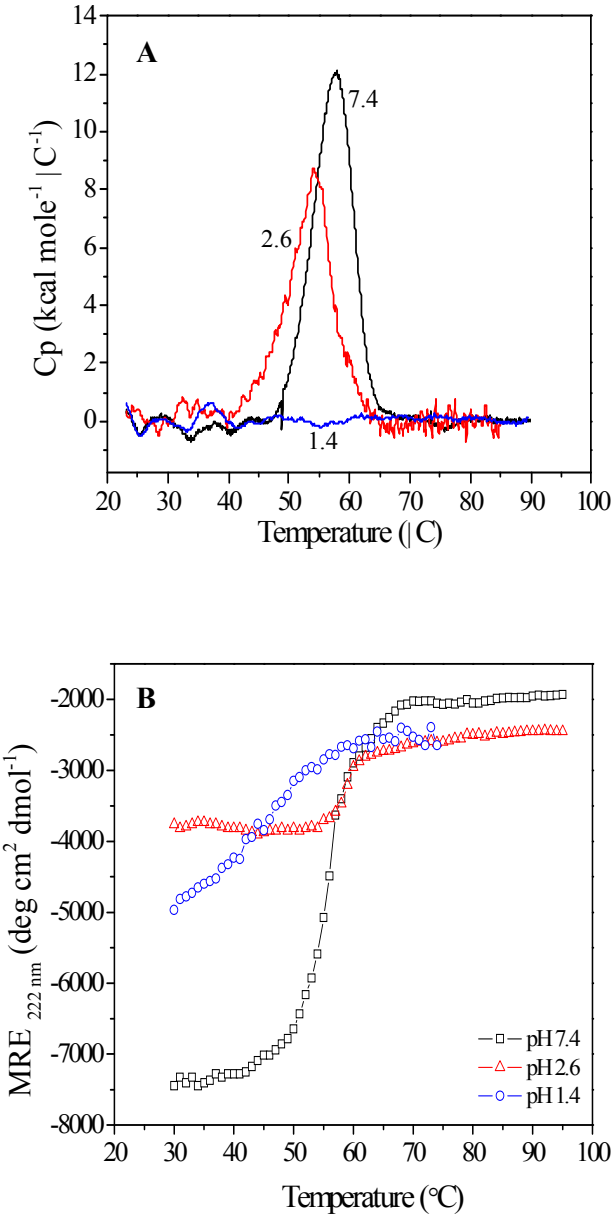

Fig. 9

Table 1 Parameters describing unfolding of CaLB at different pH values and under 6 M GuHCl denatured condition.

		Secondary structure						Tertiary structure	
State	pH	MRE $_{222\ nm}$	SS(%)	α-helix[a]	α-helix[b]	β-sheet[b]	RC[b]	MRE $_{277\ nm}$	TS(%)
Native	7.4	-7,402±125	100	32±1.0	33±1.5	16±1.2	41±1.3	68±3.1	100
	2.6	-3,606±184	48	19±1.1	20±1.2	12±1.1	66±1.4	26±2.9	62
MG	1.4	-4,968±165	67	24±1.2	23±1.4	41±1.3	32±1.4	5±2.5	7
Acid reversibility	1.0 → 7.4	-6,560±145	88	29±1.2	28±1.3	12±1.1	29±1.3	40±2.1	58
Alkali reversibility	11.0 → 7.4	-5,850±132	79	27±1.1	26±1.2	10±1.2	24±1.1	17±1.8	25
6 M GuHCl	7.4	-905±112	12	11±1.0	—	—	—	2±1.5	3

[a] % α-helix content calculated by Chen et al method [22], equation no. (2)

[b] % secondary structure content calculated from online K2D3 software

SS: secondary structure
TS: tertiary structure
RC: random coil

Table 2 Refolding yields of acid and base unfolding CaLB from the different pH values to pH 7.4. Activity at pH 7.4 taken as 100% and retained activity of refolded sample is calculated. The CaLB concentration was 6 μM.

pH	Protein recovery (%)[a]	Retained activity (%)	V_{max} (μM min^{-1})	K_m (μM)	k_{cat} (min^{-1})	k_{cat}/K_m (μM^{-1} min^{-1})
1.0	03	00	NA	NA	NA	NA
2.0	13	03	0.02	0.14×10^{4}	3.3×10^{-3}	2.3×10^{-3}
3.0	39	09	0.07	0.26×10^{4}	11.6×10^{-3}	4.4×10^{-3}
4.0	47	36	0.40	1.41×10^{4}	66.6×10^{-3}	4.7×10^{-3}
5.0	48	43	0.84	1.65×10^{4}	140×10^{-3}	8.4×10^{-3}
6.0	51	75	1.89	3.14×10^{4}	315×10^{-3}	10.4×10^{-3}
7.0	88	82	4.02	3.78×10^{4}	670×10^{-3}	16.5×10^{-3}
7.4	100	100	4.18	4.05×10^{4}	696×10^{-3}	17.1×10^{-3}
8.0	86	80	3.58	3.89×10^{4}	596×10^{-3}	15.3×10^{-3}
9.0	82	78	2.31	3.23×10^{4}	385×10^{-3}	11.9×10^{-3}
10.0	71	72	1.26	2.32×10^{4}	210×10^{-3}	9.0×10^{-3}
11.0	35	60	0.28	0.92×10^{4}	46.6×10^{-3}	5.0×10^{-3}
12.0	02	00	NA	NA	NA	NA
13.0	00	00	NA	NA	NA	NA

[a] Protein recovery calculated after re-adjusting the pH to 7.4 to check the refolding towards the native state

All measurement were carried out at 30 °C

k_{cat}/K_m; catalytic efficiency

RA; retained activity

Values of V_{max} and K_m were derived from Michaelis-Menten plot

k_{cat}; catalytic constant or turn over number ($V_{max}= k_{cat}\times$Enzyme concentration)

Table 3 Parameters describing unfolding of CaLB at different pH values by intrinsic, extrinsic and acrylamide quenching experiments.

		Intrinsic fluorescence		Extrinsic fluorescence		Acrylamide quenching	
State	pH	$FI_{322\ (nm)}$	$\lambda_{max\ (nm)}$	$FI_{480\ (nm)}$	$\lambda_{max\ (nm)}$	K_{sv} (M^{-1})	R^2
Native	7.4	1354±4.2	322±0.69	57±2.3	479±1.5	1.97±0.01	0.995
	2.6	535.2±3.4	339±0.76	67±2.2	483±1.4	2.15±0.03	0.987
Molten globule	1.4	748.5±3.8	336±0.61	915±3.8	472±1.1	2.67±0.03	0.981
6 M GuHCl	7.4	379±1.9	350±0.89	20±2.0	513±2.2	3.64±0.04	0.981

Table 4 pH dependence relationship of the hydrodynamic radii (R_h) and translational diffusion coefficients ($D_W^{25°C}$) from dynamic light scattering (DLS) experiments describing different states of CaLB. Stokes radii (R_s), molecular weight and elution volume (Ve) describing different states of CaLB obtained from size-exclusion chromatography (SEC) experiments.

		DLS				SEC		
State	pH	App. M.W. [kDa]	R_h [Å]	$D_w^{25°C}$ [$cm^2 s^{-1}$]	P_d [%]	R_s [Å]	App. M.W. [kDa]	Ve [ml]
Native	7.4	35±1.4	27±0.01	$1.79±0.02×10^{-6}$	8.0±1.5	27±0.02	34±1.4	58±0.2
	2.6	44±1.8	30±0.02	$1.71±0.01×10^{-6}$	11.3±1.4	30±0.01	44±1.2	55±0.3
Molten globule	1.4	59±1.3	34±0.01	$1.10±0.09×10^{-6}$	11.9±1.2	36±0.02	69±1.3	50±0.4
6 M GuHCl	7.4	90±1.5	41±0.03	$5.93±0.18×10^{-7}$	13.3±1.3	51±0.04	151±1.6	41±0.3

All measurement were carried out at 25 °C

App. M.W; apparent molecular weight

P_d; polydispersity index

R_h; hydrodynamic radii calculated from equation no. (9)

R_s; Stokes radii calculated from equation no. (10)

Ve; elution volume

Table 5 Thermodynamic parameters derived from GuHCl induced unfolding for the conformational stability of CaLB at pH 7.4, 2.6 and 1.4.

Methods/parameters	pH 7.4	pH 2.6	pH 1.4
GuHCl unfolding CD at $_{222\ nm}$	Cooperative	Cooperative	Non-cooperative
C_m (M)	1.08±0.03	1.40±0.02	1.76±0.03
ΔG_u^o (kcal mol^{-1})	7.72± 0.29	12.39±0.23	15.09±0.37
m-value (kcal mol^{-1} M^{-1})	7.15± 0.21	8.83± 0.57	8.55±0.31
GuHCl unfolding FI at $_{322\ nm}$	Cooperative	Cooperative	Non-cooperative
C_m (M)	0.56±0.03	1.35±0.02	1.51±0.01
ΔG_u^o (kcal mol^{-1})	12.26± 0.61	15.77±0.43	17.08±0.82
m -value (kcal mol^{-1} M^{-1})	21.89±1.08	11.65±0.83	11.3± 0.02

The data are the average and standard deviation of at least four sets of experiments. The protein concentrations were used 6 μM for GuHCl unfolding.

Table 6 Kinetic constants of refolding of CaLB after the burst phase at various GuHCl concentration at pH 7.4.

GuHCl concentration	k_{fast}	k_{slow}	$t_{1/2fast}$	$t_{1/2slow}$
1.0 M	1.32	4.00	0.53	0.17
2.0 M	0.93	2.78	0.75	0.25
4.0 M	0.68	2.08	1.01	0.33

k = rate constant expressed in s^{-1}
$t_{1/2}$ = half time of decay expressed in s

Table 7 Thermodynamic parameters for the thermal unfolding of CaLB measured by DSC and MRE $_{222\ nm}$. The protein concentrations were used 10 and 6 μM for thermal unfolding by DSC and far-UV CD measurements.

Technique/parameters	pH 7.4	pH 2.6	pH 1.4[§]
DSC			
T_m	57.9±0.01	54.1±0.02	-
ΔH_{cal}	101±0.38	78±0.50	-
ΔH_{vH}	104±0.49	89±0.72	-
R	1.0	1.1	-
MRE $_{222\ nm}$	Cooperative	Cooperative	Non-cooperative
T_m (°C)	57±0.8	53±0.6	-
ΔG_u^o	10.55±0.5	19.9±0.2	-

[§]Thermogram not generated
R=$\Delta H_{vH}/\Delta H_{cal}$
T_m is expressed in °C
ΔG_u^o and ΔH are expressed in kcal mol^{-1}